

Blue Straggler Stars in Old Open Clusters and the Kraft Break

EVAN LINCK ¹ AND ROBERT D. MATHIEU ¹

¹*Department of Astronomy, University of Wisconsin-Madison, 475 N. Charter St., Madison, WI 53706, USA*

(Received 2026 April 17; Revised 2026 May 12; Accepted 2026 May 14)

ABSTRACT

We measure the projected rotational velocities ($v \sin i$) of the solar-like blue straggler stars (BSSs) in the old (≥ 4 Gyr) open clusters M67, NGC 188, and NGC 6791. We find that the BSS rotation distribution shows a Kraft break similar to that found in the field. The main-sequence progenitors of these BSSs were cooler than the Kraft break and have spun down by their age. The binary interactions that create BSSs are expected to spin up these progenitors, so current BSS rotation rates are due to transformation and any subsequent spin-down. We observe that BSSs hotter than the Kraft break are rapidly rotating, showing that binary evolution spins up these, and likely all, BSSs to initial rotational periods below two days—still below critical velocity. BSSs below the Kraft break currently have slow rotation rates, and those within the Kraft break have a mixture of rotation rates suggesting rotational transition. This dependence of rotation on effective temperature indicates that BSS envelopes behave like those of single stars, becoming convective and generating magnetic fields at the same temperatures. For globular cluster BSSs with $[\text{Fe}/\text{H}] \sim -1.5$, we find evidence of a BSS rotation transition region that is 100–250 K hotter than at solar metallicity. We find the $v \sin i$ distributions of BSSs in open clusters have similar characteristics to both high- and low-density globular clusters, indicating the density of environment is not the only factor that can determine rotational distributions. We suggest that velocity dispersion plays an important role.

1. INTRODUCTION

Blue straggler stars (BSSs) in star clusters are bluer, and often brighter, than the main-sequence turn-off (MSTO) of their host cluster. Their position on a color-magnitude diagram (CMD) indicates that they can be many tenths of a solar mass more massive than other cluster stars (e.g., E. M. Leiner & A. Geller 2021; V. V. Jadhav & A. Subramaniam 2021; R. D. Mathieu & O. R. Pols 2025; E. Linck & R. D. Mathieu submitted 2026). BSSs form after gaining mass through an interaction within binary stars via mass transfer, merger, and collisions (W. H. McCrea 1964; N. Andronov et al. 2006; P. J. T. Leonard 1989). Each of these formation pathways is expected to spin-up the mass-gaining star (M. Sun et al. (2024a); F. R. N. Schneider et al. (2019); A. Sills et al. (2002)). In the mass-transfer scenario, a major challenge is that so much angular momentum is predicted to be transferred by even only a few hundredths of a solar mass of material that BSSs will be spun-up to critical velocity, at which point they stop accreting material (W. Packet 1981; E. Matroziis et al. 2017; M. Sun et al. 2024a).

Rotation is a critical diagnostic for many stellar processes. For stars with convective envelopes—those within and cooler than the Kraft break (R. P. Kraft

1967), magnetic braking provides a mechanism to spin a star down (S. Gossage et al. 2023), provided they have convective envelopes that yield efficient magnetic braking. The efficiency of magnetic braking has a complex relationship between the rotation rate of the star and the convective turnover time—which in turn is a function of the depth of the convective zone and has an empirical dependence on $[\text{Fe}/\text{H}]$, T_{eff} , $\log g$, stellar evolution phase, and color (A. M. Bonanno et al. 2025). Whether a star has a convective envelope is set by the opacity of the outer layers of a star due to ionization zones, which is metallicity and temperature dependent, and the steepness of the temperature gradient needed to transport energy through the envelope. Roughly, solar-metallicity stars less massive than $1.35 M_{\odot}$ will develop large enough convective envelopes for spin-down over the course of several hundred Myr to a few Gyr. Magnetic braking enables gyrochronology, which links low-mass-star rotation rates with their ages (S. A. Barnes 2003; R. Angus et al. 2019; L. G. Bouma et al. 2023).

BSSs have been found to be rapidly rotating in a wide variety of environments, including the field (e.g., G. W. Preston & C. Sneden 2000; B. W. Carney et al. 2005), open clusters (e.g., E. Leiner et al. 2018; E. Linck et al. 2024), and globular clusters (e.g., F. R. Ferraro et al. 2023). Here we study the distribution of BSS rotation rates in the open clusters M67, NGC 188, and NGC 6791 as a function of effective temperature (T_{eff}).

This work is the companion paper to [E. Linck & R. D. Mathieu](#) (submitted 2026, hereinafter Paper 1), in which we investigated the stellar properties of BSSs in six old open clusters (> 4 Gyr), including the three here, using their CMD locations. Here, we build on those BSSs and their properties. In Section 2, we first measure the projected rotational velocities ($v \sin i$) of the BSSs. In Section 3, we examine the relationships of both $v \sin i$ and rotation periods with T_{eff} and discuss the implications of the results for angular momentum transfer during the interaction, BSS stellar structure, and gyrochronology. In Section 4, we compare our open cluster findings to similar studies in globular clusters and explore the metallicity, density, and velocity dispersion dependencies of the $v \sin i$ distribution. Finally, we summarize our findings in Section 5.

2. BSS SAMPLE AND MEASUREMENTS

We examined the $v \sin i$ of BSSs in three old open clusters with MSTO masses $< 1.3 M_{\odot}$ that are well-studied by the WIYN Open Cluster Study (WOCS; [R. D. Mathieu 2000](#)): M67 (4.1 Gyr), NGC 188 (6.6 Gyr), and NGC 6791 (8.6 Gyr). Notably, main-sequence stars in these old clusters are both cooler than the Kraft break, meaning they have an efficient mechanism for spin-down, and old enough to have spun down ([L. G. Bouma et al. 2023](#)). Given this spin-down of the BSS progenitors in these clusters, the rotation rates of present-day BSSs should be due to the binary interactions that created them and any subsequent spin-down.

This work uses the membership lists, isochrone fits, and BSSs identified and characterized (including T_{eff} , radius, and errors) in Paper 1. BSS and other cluster member star properties were derived using Gaia DR3 G, BP, RP photometry ([Gaia Collaboration et al. 2023](#)) and single-star MIST models (Version 1.2, [A. Dotter 2016](#); [J. Choi et al. 2016](#); [B. Paxton et al. 2011, 2013, 2015](#)). Figure 1 shows the CMDs of each cluster, the $v \sin i$ of member stars, and the BSSs of each cluster. See Appendix A for BSS IDs, properties, and $v \sin i$ measurements.

The WOCS radial-velocity survey has made extensive time-series spectroscopic measurements of all stars on the upper main sequence and brighter for M67 and NGC 188 ([A. M. Geller et al. 2021](#); [R. S. Narayan et al. 2026](#)) and most stars from the MSTO and brighter for NGC 6791 ([B. M. Tofflemire et al. 2014](#)). These measurements were made with the WIYN 3.5m Hydra Multi-Object Spectrograph ($R \sim 20,000$).²

Following the procedure of [K. L. Rhode et al. \(2001\)](#), $v \sin i$ is measured through the IRAF task `fxcor` ([M. J. Fitzpatrick 1993](#)), which calculates the cross-correlation

function (CCF) between observed spectra and an observed solar template spectrum. To calibrate the relationship between $v \sin i$ and CCF full-width half-maximum (FWHM), we used artificially spun-up solar spectra, made by convolving our observed solar template with rotational profiles at specific $v \sin i$ up to $v \sin i = 150 \text{ km s}^{-1}$ ([A. M. Geller et al. 2010](#)). These spun-up templates were then cross-correlated with the observed template to define the relationship between $v \sin i$ and CCF FWHM. Above $v \sin i = 10 \text{ km s}^{-1}$, the FWHM strongly correlates with $v \sin i$. However, the relationship flattens below $v \sin i = 10 \text{ km s}^{-1}$ due to the spectral resolution limit; we take this as our measurement floor.

For stars with multiple spectra (almost every BSSs in NGC 188 and M67 have > 10 observations and those in NGC 6791 that we have observed have at least 3), we take the median $v \sin i$. FWHM measurements are consistent across these multiple spectra (usually within 2%), especially for stars with $v \sin i < 80 \text{ km s}^{-1}$. We estimate errors on $v \sin i$ to be $< 2 \text{ km s}^{-1}$ for these stars, although errors rise rapidly above this to $\sim 10 \text{ km s}^{-1}$ for $v \sin i = 120 \text{ km s}^{-1}$.

For this work, we adopt the definition of fast rotating stars of [F. R. Ferraro et al. \(2023\)](#): $v \sin i \geq 40 \text{ km s}^{-1}$. Due to our measurement lower limit, we categorize slow rotators as those with $v \sin i \leq 10 \text{ km s}^{-1}$. Intermediate rotators are between those limits.

[A. C. Nine et al. \(2024\)](#) has measured the $v \sin i$ of many of the BSSs in M67; our measurements agree to within $\sim 5 \text{ km s}^{-1}$ of theirs. APOGEE-2 has made $v \sin i$ measurements of 9 of our BSSs (7 in M67 and 2 in NGC 188, [Abdurro'uf et al. 2022](#)); all but one of these measurements are within 5 km s^{-1} of ours (the remaining is 15 km s^{-1} higher than our measurement of 13 km s^{-1}). APOGEE-2 has measured the $v \sin i$ of WOCS 2011 in M67 to be 8.84 km s^{-1} , which we adopt for this study. Although there are some differences in the $v \sin i$ measured for these stars, each of these studies agrees that the same sets of stars are rapidly or slowly rotating.

Tidal forces will impact the rotation of close binaries. We follow the method of [E. Leiner et al. \(2019\)](#), removing any stars with known orbital periods less than twice the empirical tidal synchronization limit of ~ 30 days ([J. C. Lurie et al. 2017](#)): WOCS 4003 and 1007 in M67; WOCS 4230 and 5078 in NGC 188; and WOCS 54008 in NGC 6791. We further remove WOCS 2009 in M67 and WOCS 5885 in NGC 188 due to inability to measure photometric T_{eff} given multiple bright members in the systems.

3. BSS ROTATION IN OLD OPEN CLUSTERS

We measure the numbers of fast, intermediate, and slow rotators in each cluster: M67, 7 ($44 \pm 17\%$), 5 ($31 \pm 14\%$), and 4 ($25 \pm 12\%$); NGC 188, 5 ($26 \pm 12\%$), 2 ($11 \pm 7\%$) and 12 ($63 \pm 18\%$); NGC 6791, 4 ($13 \pm 6\%$), 2 ($6 \pm$

² The WIYN 3.5m Observatory is a joint facility of the University of Wisconsin–Madison, Indiana University, NSF’s NOIRLab, the Pennsylvania State University, and Princeton University.

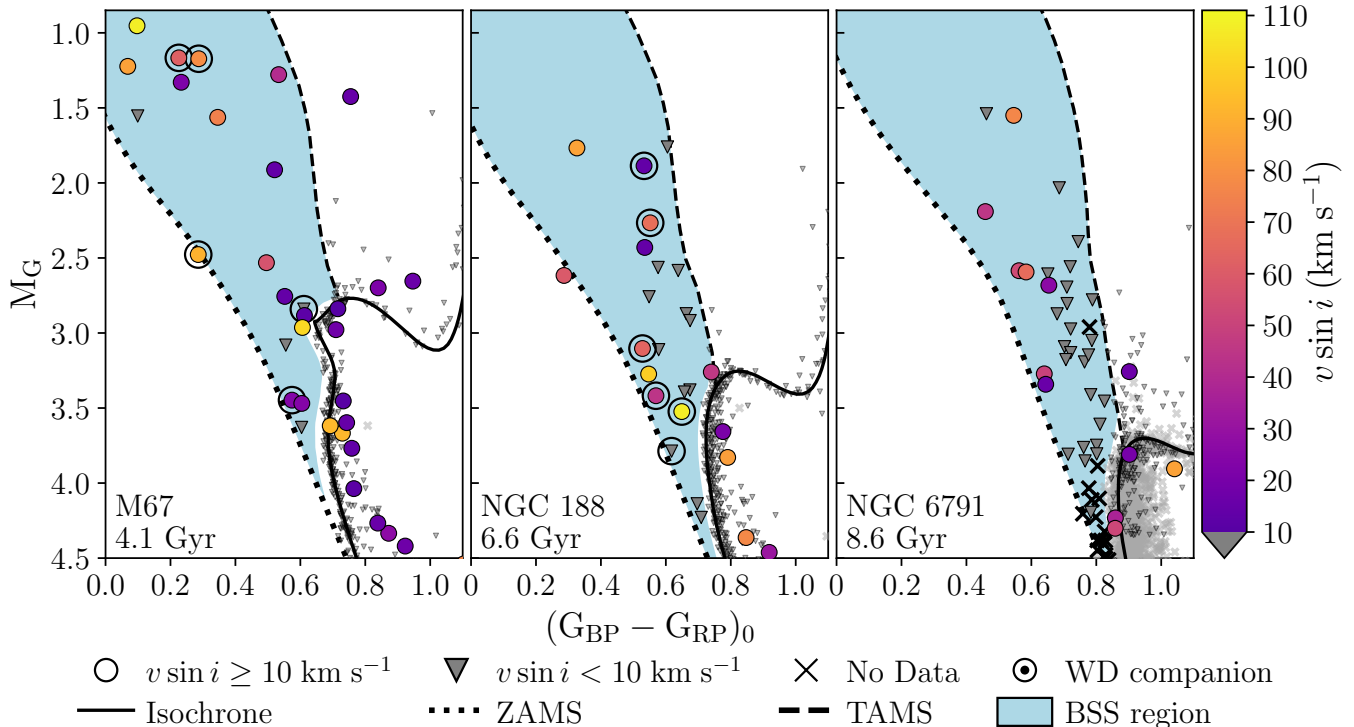


Figure 1. The BSS and upper main-sequence regions of the M67, NGC 188, and NGC 6791 CMDs. The BSS regions—bounded by the isochrone (solid line), ZAMS (dotted line), and TAMS (dashed line) found in Paper 1—are denoted by the blue areas. Stars with $v \sin i$ measurements above our floor of 10 km s^{-1} are marked with color-coded circles; stars with measured $v \sin i$ below our floor are marked with downward triangles; stars without $v \sin i$ measurements are marked with black Xs. Non-BSSs that are slowly rotating or are lacking data are shown at a smaller scale for visual clarity of the main sequence. Stars with a ring around the central point have a known WD companion.

5%), and 25 ($81 \pm 16\%$), respectively. We note that the fraction of fast rotators decreases with cluster age.

3.1. Temperature Distribution of $v \sin i$

In Figure 1, we observe that the fastest rotating stars are at bluer colors than slower rotating stars. At colors bluer than $\text{BP} - \text{RP} = 0.6$, BSS $v \sin i$ are as high as 110 km s^{-1} . At colors redder than $\text{BP} - \text{RP} = 0.6$, most BSS $v \sin i$ drop below our measurement floor.

We plot T_{eff} versus $v \sin i$ in Figure 2. The $v \sin i$ distribution naturally divides into three distinct regions: below 6300 K, all of the BSSs have $v \sin i \leq 10 \text{ km s}^{-1}$; between 6300 K and 6750 K, the BSSs show a mix of rotation rates; and above 6750 K all but two of the BSSs are measurably rotating. We also identify BSSs with known WD companions (N. M. Gosnell et al. 2015; N. Sindhu et al. 2019; V. V. Jadhav et al. 2019; N. M. Gosnell et al. 2019; E. Leiner et al. 2018; N. Vernekar et al. 2023; A. C. Nine et al. 2023; H. Pal et al. 2024).

First, we examine the 11 hottest BSSs ($T_{\text{eff}} > 6750 \text{ K}$) without close companions. The 9 measurably rotating stars have an average $v \sin i$ of $75 \pm 8 \text{ km s}^{-1}$ ($\sigma = 24 \text{ km s}^{-1}$). Assigning each star the median inclination angle ($i = 60^\circ$) gives $\bar{v}_{\text{rot}} = 87 \pm 9 \text{ km s}^{-1}$. The two stars that have $v \sin i \leq 10 \text{ km s}^{-1}$ (NGC 6791: WOCS 4003;

M67: WOCS 2011) are among the hottest and most massive stars in each cluster. Using a Monte Carlo simulation to estimate the true distribution of $v \sin i$ from our mean $v \sin i$ and error at $i = 60^\circ$ as the mean v_{rot} of rotators and a random uniform distribution of the cosine of the inclination angle, we find $p = 7\%$ that 1 star of 11 has a $v \sin i < 10 \text{ km s}^{-1}$, but $p = 0.2\%$ that 2 stars do. This means that in general, the $v \sin i$ distribution of the hottest BSSs are consistent with a population in which all BSSs are rapidly rotating, although an exception or two may exist. Examining the population below 6300 K shows that none are measurably rotating, let alone rapidly rotating. Finally, the population between 6300 and 6750 K shows a mix of rotation rates, with a trend to lower rotation rates at cooler temperatures.

These divisions align closely with the well-known Kraft break. In the literature, the division between hot and cold stars (those with or without a convective envelope) is frequently given as $T_{\text{eff}} \sim 6200 \text{ K}$ without citation. In a recent empirical study of rotation rates of nearby field stars, A. C. Beyer & R. J. White (2024) found stars with T_{eff} between 6450 and 6650 K to have a mixture of rapidly rotating and slowly rotating stars and labeled this temperature domain as the Kraft break. We plot this region in Figure 2 for reference and note

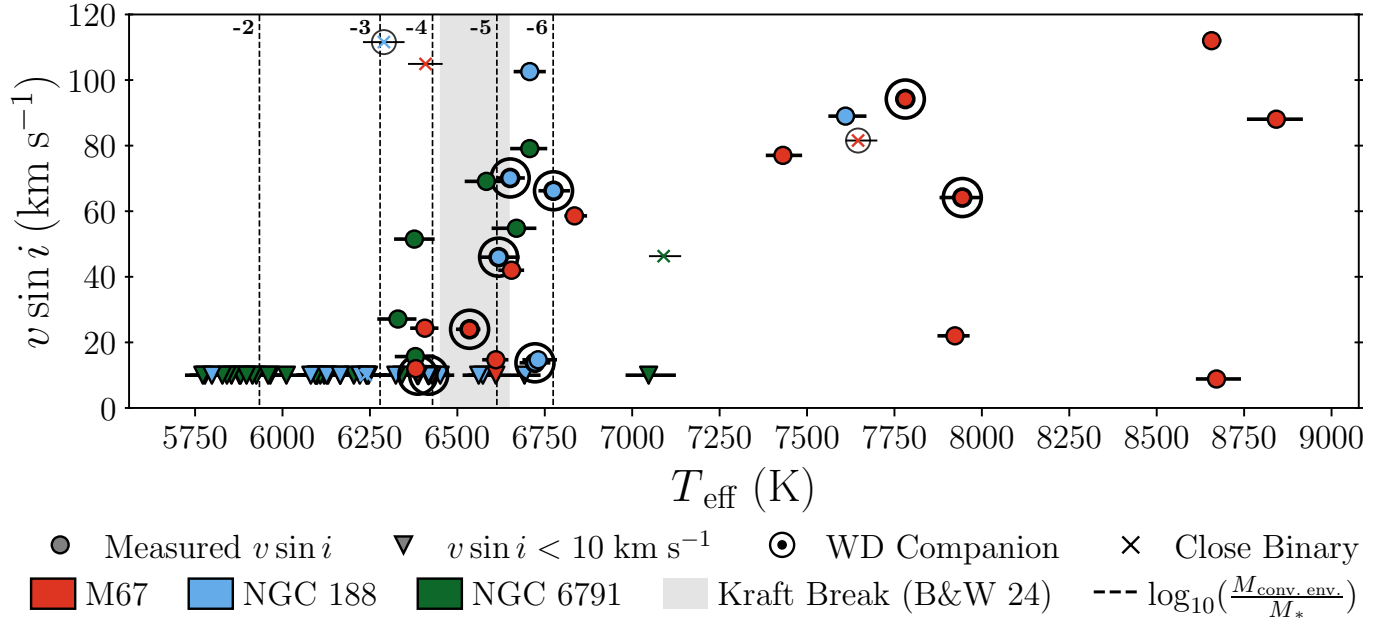


Figure 2. The BSS $v \sin i$ distribution by effective temperature, color-coded by cluster (M67: red, NGC 188: blue, NGC 6791: green). BSSs used in the analyses in this work with a measured $v \sin i$ are marked by circles; those with a $v \sin i$ below our floor of 10 km s^{-1} are marked with triangles at their upper limit. BSSs that have been discarded due to an orbital period less than 40 days are marked with an X. BSSs without a $v \sin i$ measurement are not plotted. Finally, BSSs with a known WD companion have a ring around their central point. Three distinct populations are apparent: cool stars that are all slowly rotating, hot stars that are primarily rapid rotators, and a population in between with a mixture of rotation rates. This final group are stars with thin convective envelopes that will spin-down, but slower than cooler stars with thick convective envelopes. For reference, we plot a dashed line at the maximum T_{eff} at which the mass fraction of a convective envelope decreases by an order of magnitude among our MESA models. The region of a mixture of BSS rotation rates and thin convective envelopes aligns well with the empirical Kraft break region of A. C. Beyer & R. J. White (2024, plotted as the grey-shaded area from 6450–6650 K), although is both cooler and hotter (roughly 6215–6750 K).

that although it demarcates the area where BSS rotation rates are changing, there are BSS fast rotators that are somewhat cooler than this region and BSS slow rotators that are somewhat hotter than this region.

C. Spalding & J. N. Winn (2022) used a limit of the convective envelope accounting for 3×10^{-3} of the total mass fraction of a star to identify the lower boundary of the Kraft break; we follow a similar approach here. In Paper 1, we used Modules for Experiments in Stellar Astrophysics (MESA; version 24.03.01 B. Paxton et al. 2011, 2013, 2015, 2018, 2019; A. S. Jermyn et al. 2023) to model main-sequence solar-metallicity stars. We used MESA’s predictive mixing algorithm with the Ledoux criterion. In Figure 2, we show the T_{eff} at which mass fractions of the convective envelopes of solar-metallicity main-sequence stars with masses between 1 and $1.5 M_{\odot}$ decrease by orders of magnitude. At $T_{\text{eff}} \sim 6750 \text{ K}$, the convective envelopes rapidly decline with increasing temperature by several orders of magnitude and becomes negligible.

The T_{eff} region of mixed BSS rotation rates maps very well to the decreasing mass fractions of convective envelopes. Among BSSs near the Kraft break, the coolest measurably rotating BSS has $T_{\text{eff}} = 6330 \text{ K}$ and the

hottest slowly rotating BSS has $T_{\text{eff}} = 6690 \text{ K}$. For specificity, we identify the BSS Kraft break as spanning T_{eff} of $6200 - 6750 \text{ K}$ and Gaia BP-RP of $0.66 - 0.52$, the T_{eff} domain where the mass fraction of the convective envelope falls from 10^{-3} to 10^{-6} . This may generalize to the Kraft break for field stars.

This in turn provides the explanation of the three rotation-rate populations among the BSSs. BSSs below the Kraft break have thick convective envelopes, providing an efficient mechanism for spin-down. BSSs that are above the Kraft break do not have an efficient mechanism to spin down and thus maintain their post-interaction rotation rate. BSSs within the Kraft break have thin convective envelopes that allow them to spin down, but do so slowly. This can be further seen across this region as the fastest rotators are at the hottest temperature, indicating that they have the thinnest convective envelopes that would take the longest to spin down.

In Paper 1, we found that the bluer BSSs formed within the last 1–2 Gyr. Redder BSSs had less restriction on their time as a BSS, but in M67 and NGC 188 generally had transformed in the last 1–4 Gyr, whereas most in NGC 6791 must have transformed within last 5 Gyr. The youngest age that these clusters could have

been at the times when their current BSSs formed is about 2 Gyr, roughly the present age of NGC 6819 (2.5 Gyr), although most of the BSSs have formed more recently (including many within the last Gyr). Examining the MIST temperatures and rotation rates (L. G. Bouma et al. 2023; P. R. Van-Lane et al. 2025) of main-sequence stars in NGC 6819 and M67 shows that the progenitor main-sequence stars of most, if not all, of the BSSs would have low-enough T_{eff} to have convective envelopes and be old enough to have spun down to periods greater than 10 days by the time of the interaction. This means that the BSS rotation rates are due to the spin-up of the interaction and any subsequent spin-down due to magnetic braking.

There are several important implications of these observations. The first is that almost all of the BSSs that do not have an efficient spin-down mechanism are rapidly rotating, despite their progenitor accretors having previously spun down, indicating that BSSs are indeed spun-up during their interactions. Second, in order to exhibit the same $v \sin i - T_{\text{eff}}$ distribution of single stars, BSSs must develop convective envelopes at the same temperatures that single stars do, indicating that their surface structure is similar to a star undergoing normal single-star stellar evolution despite having accreted material. This finding matches that of E. Leiner et al. (2018) in lower-mass interaction products with known WD companions—including several of the BSSs in NGC 188—that spun down following the gyrochronology relationships of low mass stars, which we explore in the next subsection. Third, the fraction of fast rotators BSSs tracks the fraction of BSSs in and above the Kraft break, which is a consequence of the MSTO mass (and thus whether progenitors would have spun down) and BSS masses of a given cluster age. Thus, old clusters have fewer fast rotators.

3.2. BSS Rotation Periods

In the previous sub-section, we saw a striking relationship between $v \sin i$ and T_{eff} among the BSSs. In order to compare these results to other observational and theoretical studies (e.g., E. Leiner et al. 2018; A. C. Nine et al. 2023; M. Sun et al. 2024a), rotational periods are needed.

Direct measurements of rotational periods of BSSs in open clusters through photometric light curves can be challenging as the dense environments can pollute light curves with signals from neighboring stars (e.g., TESS pixels are 21 arcsec on a side). Further, the hottest BSSs in old open clusters are A- and early F-type stars, and less than one-third of A-type stars show rotational signatures (e.g., starspots) in their light curves (L. A. Balona 2011). Both M67 and NGC 6791 were observed by the Kepler spacecraft; several of the BSSs in these clusters have published rotation periods from these observations (E. Leiner et al. 2019; S. Sanjayan et al. 2022). NGC 188 has been observed by TESS and light curves are

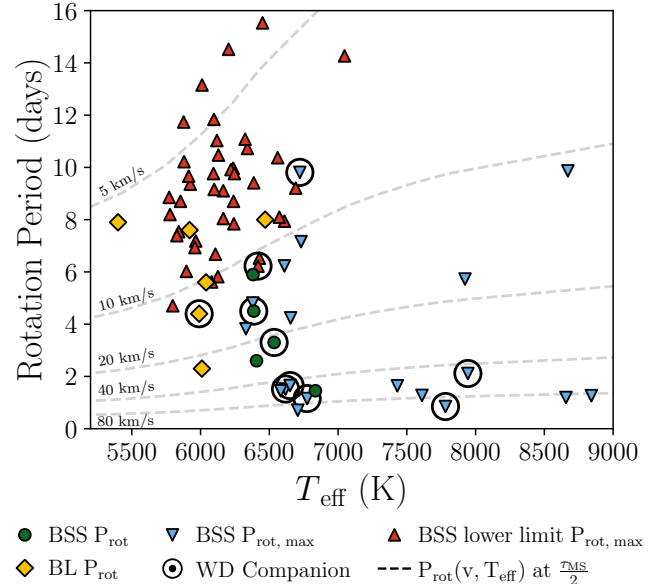


Figure 3. The rotation periods of the BSSs and BLs by T_{eff} . BSSs and BLs with known rotation periods are plotted with green circles and yellow diamonds, respectively. BSSs with measured $v \sin i$ have a maximum rotation period and are plotted with downward blue triangles. BSSs with $v \sin i < 10 \text{ km s}^{-1}$ have a known lower limit on maximum rotation period and are plotted with upward red triangles. Using MIST evolutionary tracks, we mapped the T_{eff} of main-sequence stars that are halfway through their main-sequence lifetimes to their radii at that time. We can then calculate the rotation period of these stars for a given equatorial velocity (i.e., $v \sin i$ at an inclination of 90°); we show these velocities as dashed lines. The radius of a star grows throughout its main-sequence lifetime, so these lines will shift lower for a star that is closer to the ZAMS and higher for a star closer to the TAMS.

available for some stars through differential image subtraction (L. G. Bouma et al. 2019), but to our knowledge no rotation periods of BSSs have been published.

For most of the BSSs, we use $v \sin i$ values measured here and radii from Paper 1 to derive maximum rotation periods (due to $\sin i$). The $v \sin i$ -derived maximum periods are consistent with the rotation periods of the BSSs found through light curves. For stars with $v \sin i \geq 10 \text{ km s}^{-1}$, we can put a specific upper limit on the rotation period. For stars with $v \sin i < 10 \text{ km s}^{-1}$, we can put a lower limit on the maximum period. We show the distribution of the BSS rotation periods with T_{eff} in Figure 3 and mark stars that have hot WD companions.

Blue lurkers (BLs) are mass-gaining stars embedded among the main sequences of clusters. These stars were first identified by E. Leiner et al. (2019) in M67 due to their anomalously fast rotation periods (from light curves) despite being in long-period binaries, which indicates they were spun-up during a binary interaction.

These stars are BSSs that did not gain sufficient mass to stand apart from other main-sequence stars in CMDs (R. D. Mathieu & O. R. Pols 2025). We also show them on Figure 3. (We note that none of the BLs of M67 have measured $v \sin i > 10 \text{ km s}^{-1}$.)

The most rapidly-rotating BSSs at effective temperatures in and above the Kraft break have rotation periods below 2 days. None of these stars have equatorial velocities near critical velocities (350–450 km s^{-1} for these masses and radii). At most the rapid rotators are rotating at speeds about a quarter of critical velocity.

It is of interest to compare the BSS rotation periods to empirical spin-down times (L. G. Bouma et al. 2023). BSSs with $6000 < T_{\text{eff}} \lesssim 6200$ have a lower limit on maximum period greater than 6 days. Empirical rotation periods of stars in this temperature range increase quickly during the first 500 Myr from 1–2 days to about 4–6 days before the rate of change dramatically slows down. By 2.5 Gyr, stars in this temperature range have rotation periods of 7–10 days. Presuming initial rotation periods of ~ 1 day as observed for the hotter BSSs, these cool BSSs with rotation periods of 7–10 days have transformation ages greater than 2 Gyr. These cool BSSs are low-mass BSSs in either of NGC 188 or NGC 6791 (Figure 2). As shown in Paper 1, many of the low-mass BSSs in NGC 188 do in fact have transformation ages permitting these spin-down timescales. Presumably this is also true in the even older NGC 6791.

An alternative approach is comparison of spin-down times with the transformation ages of the BSSs with known WD companions (all have cooling ages of $\lesssim 600$ Myr). Unfortunately, all such BSSs except the BL with a hot WD (E. M. Leiner et al. 2025) are above the temperatures at which spin-down rates have been modeled (e.g., $T_{\text{eff}} < 6200 \text{ K}$, L. G. Bouma et al. 2023). E. M. Leiner et al. (2025) found the WD companion of the BL to have a cooling age of 400 Myr. The BL rotation period of 4.4 days agrees well with the spin-down models of L. G. Bouma et al. (2023). Most of the BSSs with WD companions that are in the Kraft break have short periods ($\lesssim 4$ days), which is consistent with their young transformation ages. However, two of these BSSs have longer (6–10 day) maximum rotation periods. Low inclination angles could explain both of these stars; light curves are needed to confirm these slow periods.

Lastly, there are some slowly rotating BSSs (without known WD companions) in and above the Kraft break (lower limit on $P_{\text{rot,max}} > 10$ days and hotter than 6200 K). Inclination angle may explain some of these stars. These stars do have larger radii (all larger than $2 R_{\odot}$) and most are near the ends of their main-sequence lifetimes (Paper 1 and Appendix A). The combination of increasing radii post-interaction and longer times as BSSs may have further spun them down.

The findings in this section pose issues for the possibility of gyrochronology with BSSs in many clusters. In old open clusters, many of the BSSs are cool enough to

have thin convective envelopes and spin down. M. Sun et al. (2024a) modeled post-interaction products of $1.2 M_{\odot}$ and lower and found that they did spin down and explained the rotation distribution found by E. Leiner et al. (2018). However, in open clusters younger than 4 Gyr, the mass of a star at the MSTO is above $1.3 M_{\odot}$, meaning that most of the BSSs in these clusters are going to be hotter than the Kraft break.

4. COMPARISON TO BSS ROTATION RATES IN GLOBULAR CLUSTERS

F. R. Ferraro et al. (2023) compiled $v \sin i$ measurements of BSSs ($1.1\text{--}1.5 M_{\odot}$) in eight globular clusters and found that fast rotating BSSs preferentially occurred in less dense globular clusters. The authors argue that the difference in BSS rotation rates is indicative of recent (< 1 Gyr) BSS formation via mass transfer in the low-density clusters and past collisions (at least 1–2 Gyr ago) in high-density clusters (or that collision products have undefined very efficient spin-down mechanisms).

In this section we compare the rotation rate distribution with the T_{eff} of BSSs in open clusters to those of these globular clusters. The globular clusters included and their $v \sin i$ source papers (along with the fraction of rapidly rotating BSSs from F. R. Ferraro et al. 2023) are the low-density clusters M55 (0.47, A. Billi et al. 2024), NGC 3201 (0.28, A. Billi et al. 2023), ω Centauri (0.41, A. Mucciarelli et al. 2014), and M4 (0.40, L. Lovisi et al. 2010); and the dense clusters 47 Tucanae (0.47, F. R. Ferraro et al. 2006), M30 (0.06, L. Lovisi et al. 2013b), NGC 6752 (0.0, L. Lovisi et al. 2013a), and NGC 6397 (0.13, L. Lovisi et al. 2012).³ We also include the $v \sin i$ data from the high density globular cluster NGC 1851 (A. Billi et al. 2026), which has a reported floor on $v \sin i$ of 15 km s^{-1} . Several stars in ω Centauri, 47 Tucanae, and M30 have been identified as contact binaries (A. Mucciarelli et al. 2014; F. R. Ferraro et al. 2023). As with the open clusters above, we remove these from our analyses.

4.1. The Influence of Metallicity on BSS Rotation Distributions

Metallicity changes the opacity profile of a star (L. Amard et al. 2019; L. Amard & S. P. Matt 2020). C. Spalding & J. N. Winn (2022) found evidence for a metallicity-dependent ($-0.3 < [\text{Fe}/\text{H}] < 0.3$) Kraft break that increased in T_{eff} at lower metallicity among the stellar obliquities of systems with hot Jupiters. L. Amard et al. (2020) showed that the rotation rates of high-metallicity stars were slower than low-metallicity stars in the Kepler field. Notably, A. C. Beyer & R. J. White (2024) did not find evidence of a metallicity-dependent Kraft break above and below the median

³ $v \sin i$ information was available at http://www.cosmic-lab.eu/Cosmic-Lab/BSS_rotation_catalogs.html

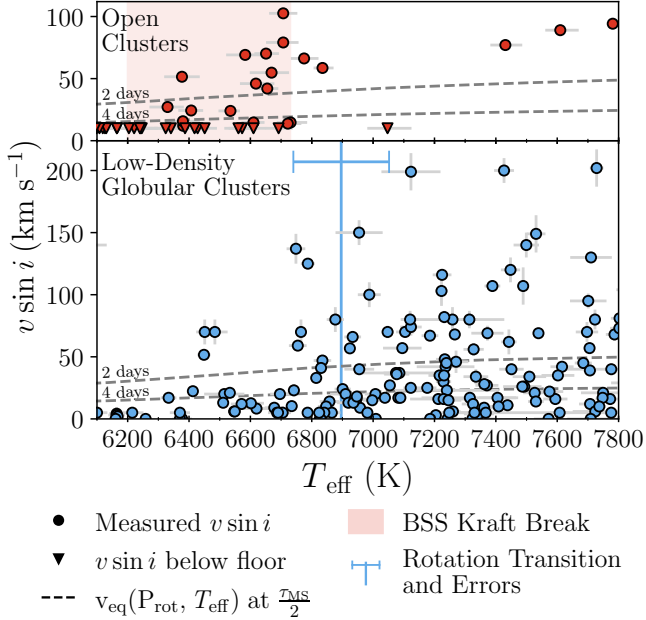


Figure 4. We show the $T_{\text{eff}}-v \sin i$ distribution of BSSs in open clusters (upper panel, in red, from Figure 2) and low-density globular clusters (lower panel, in blue). Like in Figure 3, using MIST evolutionary tracks, we calculated the equatorial velocity for stars that are half-way through their main-sequence lifetimes at a specific T_{eff} with rotational periods of 2 and 4 days, and plot these with dashed lines. We further show the BSS Kraft break at solar metallicity (red area) in the upper panel and the best-fit T_{eff} with errors (blue line) that demarcates a transition of the globular cluster BSS rotation distribution in the lower panel.

metallicity of their field-star sample ($[\text{Fe}/\text{H}] = -0.43$), but they note their sample size was small. At the much lower metallicity of $[\text{Fe}/\text{H}] = -1.58$, A. Billi et al. (2023) noticed a trend between color and BSS rotation rate in the globular cluster NGC 3201, stating that this could be evidence of more massive BSSs having formed more recently or could be due to reduced convective envelopes at higher temperatures. Here, we examine the rotation rates as a function of temperature for the BSSs in four metal-poor ($-1.2 < [\text{Fe}/\text{H}] < -1.8$) low-density globular clusters.

We derived photometric temperatures of each BSS with a $v \sin i$ measurement in M55, NGC 3201, M4, and ω Centauri from the photometry of P. B. Stetson et al. (2019) and distances of H. Baumgardt & E. Vasiliev (2021) as listed in M. Hilker et al. (2019). Stars were differentially dereddened using the average $E(B-V)$ measurements listed in W. E. Harris (1996, from which we also drew $[\text{Fe}/\text{H}]$) and differential reddening maps of E.

Pancino et al. (2024)⁴ and the bandpass reddening relations of E. F. Schlafly & D. P. Finkbeiner (2011). We used MIST to estimate a color-magnitude-temperature relationship. For each cluster (i.e., for a given $[\text{Fe}/\text{H}]$ and distance), MIST provides a tight relationship between $V - I$ color, V magnitude, and T_{eff} . To propagate photometric errors for each star, we implemented a Monte Carlo simulation that sampled from normal distributions of each star’s photometry and photometric error. We note that there are no reported errors on metallicity or average $E(B-V)$ in W. E. Harris (1996), which would also contribute to uncertainties on T_{eff} .

We plot T_{eff} and $v \sin i$ of each BSS in the bottom panel of Figure 4. Most metal-poor BSSs below $T_{\text{eff}} \sim 6750$ K are spun down. Above $T_{\text{eff}} \sim 6750$ K, the metal-poor BSSs show a broad distribution in $v \sin i$ from a few km s^{-1} to 200 km s^{-1} , including a large increase in the frequency of BSSs with $v \sin i < 50 \text{ km s}^{-1}$ ($P_{\text{rot}} > 2$ days). For comparison, we re-plot the open cluster BSSs of Figure 2 in the top panel. The rotation distribution for cooler globular cluster stars is similar to that of the open clusters and reminiscent of the Kraft break, but shifted to higher temperatures.

We created a bootstrap method to search for a T_{eff} demarcating where a shift in rotational distribution occurs. We fit a step function to the data from 6100–7800 K using a quantile regression of the median (i.e., the y -value of each step was the median in that interval) as implemented in statsmodel (S. Skipper & P. Josef 2010). For each of 500 draws, we found the T_{eff} of the discontinuity that best reproduced the data and the median of the distributions before and after the step. We found the rotation distribution changes at 6896 ± 156 K, with the median $v \sin i$ shifting from $11.5 \pm 4.3 \text{ km s}^{-1}$ below to $33.7 \pm 4.8 \text{ km s}^{-1}$ above the break.

This transition temperature is 100–250 K hotter at $[\text{Fe}/\text{H}] \sim -1.5$ than it is at solar-metallicity. We hypothesize this difference is due to metal-poor BSSs being able to undergo efficient magnetic braking at hotter T_{eff} . At this metallicity, from MIST models, the temperature range of the transition corresponds to stars of masses of 1.1 to 1.2 M_{\odot} . Because these stars are lower mass, they may be able to maintain some convective envelopes at these hotter T_{eff} than solar-metallicity stars. We suggest that this phenomena is akin to the Kraft break of metal-rich stars.

High-density globular clusters may primarily create BSSs through collisions, but mass transfer does still happen as evidenced by W UMa stars (F. R. Ferraro et al. 2023). Collision products may have different stellar structures (e.g., radiative envelopes at low mass, A. Sills et al. 2002), and so may not spin down in the same man-

⁴ Although the central region of ω Cen as having less reliable differential reddening data, we did include the 43% of BSSs in this region.

ner (A. Sills et al. 2005) as mass transfer stars, and thus not be impacted by the location of the Kraft break. Applying the same temperature-fitting procedure as above to the high-density globular clusters,⁵ we find that the few fast rotators are hotter than 7000 K, which may provide further evidence that any mass-transfer products cooler than that limit are able to spin down whereas those above cannot. For example, the T_{eff} distribution of NGC 1851 mirrors that of the open clusters, with all of the stars cooler than 7000 K slowly rotating and two-thirds of those hotter than 7000 K rotating faster than 40 km s^{-1} .

Additionally, we note that 80% of the BSSs with $v \sin i$ measurements in 47 Tuc and 72% of those in NGC 6752 are cooler than 7000 K, which could contribute to the large fraction of non-rapid rotators found by F. R. Ferraro et al. (2023) if many of these stars have an efficient spin-down mechanisms.

Two observational features noted above require further observations and modeling of the physics to understand the driving factors of the rotation distribution in metal-poor globular clusters. First, how does the interplay between metallicity, mass, and magnetic braking impact the T_{eff} of the Kraft break. For example, a metallicity dependence may have further evidence in Figure 2: the two coolest rapidly rotating BSSs are both in the metal-rich NGC 6791 ($[\text{Fe}/\text{H}] \simeq 0.35$), suggesting it may have a cooler Kraft break than M67 and NGC 188 (both of $[\text{Fe}/\text{H}] \simeq 0.0$). Second, the many high- T_{eff} low- $v \sin i$ BSSs that exist in the high-density globular clusters but do not exist in the old open clusters need to be explained. These BSSs may indicate that some difference in physical processes—such as mergers and their subsequent spin-down—is occurring between these environments.

4.2. The Influence of Density on BSS Rotation Distributions

M. Hilker et al. (2019) measured the central densities of these nine globular clusters, finding the low-density clusters to have $\log_{10} \rho_c$ ($M_{\odot} \text{ pc}^{-3}$) between 2.54 and 3.99 and the high-density clusters between 4.72 and 6.74. In comparison, the best-fit SPES models of N. Alvarez-Baena et al. (2024) give central densities for NGC 188 and M67 of $16 - 18 M_{\odot} \text{ pc}^{-3}$ and for NGC 6791 of $24 M_{\odot} \text{ pc}^{-3}$ ($1.2 < \log_{10} \rho_c$ ($M_{\odot} \text{ pc}^{-3}$) < 1.4), all an order-of-magnitude less dense than any of the globular clusters.

In Figure 5, we show the cumulative distribution functions (CDF) of $v \sin i$ for BSSs in the high- and low-density globular clusters and in the open clusters. Due to our $v \sin i$ measurement floor, values below our

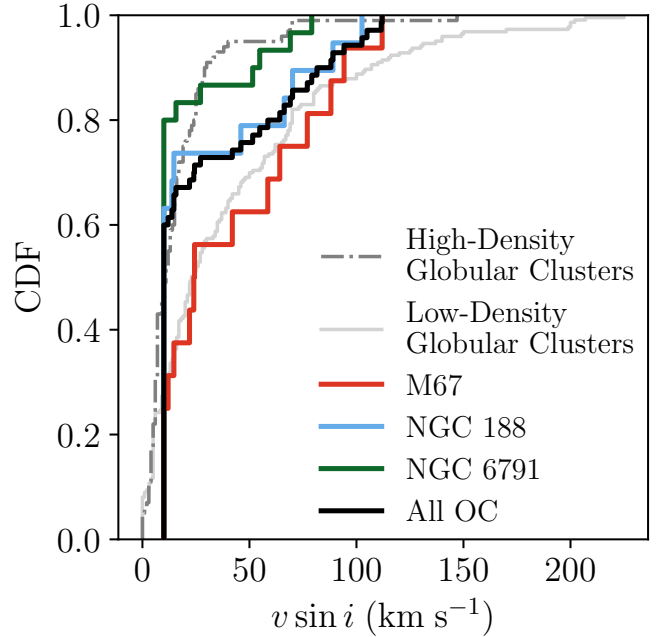


Figure 5. Comparison of the rotational velocity distributions of open and globular clusters using the empirical CDFs of three open clusters of different ages (M67: red, NGC 188: blue, NGC 6791: green, all: black) and the CDFs of (high-density and low-density globular clusters (Figure 2 of F. R. Ferraro et al. (2023))).

floor are set to 10 km s^{-1} ; we use a permutation-based Kolmogorov-Smirnov test in which values below the floor are set to 10 km s^{-1} to model a null distribution built from the data for the following statistics. Two features stand-out. First, the CDFs of M67 and NGC 6791 are statistically significantly different ($p = 0.01$), with NGC 188 splitting the difference between the two, although not statistically significantly different than either ($p \simeq 0.22$ for both comparisons). As clusters age, their MSTO and the temperatures of their BSS populations move toward lower temperatures below the Kraft break, increasing the fraction of BSSs that could spin-down. This naturally produces the observed sequence of open cluster CDFs.

Second, as an integrated ensemble, the CDF of open clusters lies between the CDFs of low-density and high-density globular clusters, even though the open cluster central densities are an order of magnitude or more smaller than either globular cluster distribution. We find that the $v \sin i$ distribution of the three open clusters combined is different than those of both the high-density clusters ($p = 0.01$) and the low-density clusters ($p = 0.01$). These p-values should be conservative as we are not considering potential larger differences in the populations below the floor.

Given that the open clusters have significantly lower densities than the globular clusters but their combined CDF lies between the lower- and higher-density globular

⁵ NGC 6397 is not in P. B. Stetson et al. (2019); we instead used the photometry listed in L. Lovisi et al. (2012) and E(B-V) of W. E. Harris (1996).

clusters, there is a suggestion in this comparison that density may not be the only factor responsible for the fraction of fast rotators in a star cluster.

4.3. *The Influence of Velocity Dispersion on BSS Rotation Distributions*

Here we suggest consideration of the role of velocity dispersion (σ) in determining BSS rotation distributions. In non-core collapse globular clusters, like in open clusters, binary mass transfer via Roche Lobe overflow has been suggested to be the primary channel to form BSSs, even in central regions (N. Leigh et al. 2007; A. Sollima et al. 2008; F. R. Ferraro et al. 2026). Binary orbital period determines the evolutionary state when an evolving star will overflow its Roche lobe (for given companion mass). In a star cluster, the local velocity dispersion sets the hard-soft orbital period for binaries (for example, A. M. Geller & N. W. C. Leigh 2015). Thus the velocity-dispersion radial profile determines the maximum orbital periods present at different cluster radii, and thereby the most-evolved state of mass-transfer progenitors. Finally, because different evolutionary states may differ in stability and conservativeness of Roche lobe overflow (RLOF), mass transfer at different evolutionary states may produce BSSs of different masses and effective temperatures. If so, this would lead to different fractions of BSSs above and below the Kraft break, and thus different BSS rotation distributions.

For specificity, we estimate the evolutionary states for mass transfer in two samples of non-core collapse globular clusters. To begin, we use MIST stellar radii for giant stars in these globular clusters (initial masses of 0.8–0.9 M_{\odot} and $-0.7 < [\text{Fe}/\text{H}] < -2$), the Eggleton approximation for the Roche lobe radius (Equation 2 of P. P. Eggleton 1983, using secondary masses of mass ratio $q = \frac{M_{\text{accretor}}}{M_{\text{donor}}} = 1$ and $q = 0.6$), and the hard-soft period boundary (equation 1 of A. M. Geller & N. W. C. Leigh 2015, using 0.3 M_{\odot} as the average mass of cluster stars). Main-sequence mass transfer may occur in systems with periods less than a few days, which would only be disrupted for $\sigma \gtrsim 50 \text{ km s}^{-1}$. For various combinations of q and $[\text{Fe}/\text{H}]$, binaries at the tip of the red giant branch (RGB) will have Roche lobe radii corresponding to orbital periods between 250 and 600 days for $18.0 \gtrsim \sigma \gtrsim 11.0 \text{ km s}^{-1}$. For thermally-pulsing asymptotic giant branch (AGB) stars at their maximum radii, orbital periods will range from 1300–1500 days for $9.5 \gtrsim \sigma \gtrsim 7.6 \text{ km s}^{-1}$. Finally, if wind RLOF (WRLOF) occurs in metal-poor binaries (C. Abate et al. 2013), WRLOF can occur in systems with periods of $10^4 - 10^5$ days (M. Sun et al. 2024b), which correspond to $2.5 \gtrsim \sigma \gtrsim 1.0 \text{ km s}^{-1}$.

The non-core collapse globular clusters of F. R. Ferraro et al. (2023) can be split into high central velocity dispersion ($\sigma_0 \geq 10 \text{ km s}^{-1}$: 47 Tuc and NGC 1851; ω Centauri $\sigma_0 \sim 18 \text{ km s}^{-1}$) and low central velocity

dispersion ($\sigma_0 \leq 5 \text{ km s}^{-1}$: M55, M4, and NGC 3201). The velocity dispersion profiles (H. Baumgardt & M. Hilker 2018) of the high- σ_0 clusters indicate that main-sequence and RGB RLOF should dominate BSS production near the cores, whereas BSSs can be formed by RLOF from all evolutionary states in the envelopes of high- σ_0 clusters. Binaries from all evolutionary states also form by RLOF at all radii in the low- σ_0 clusters. WRLOF only occurs at the outermost radii of globular clusters.

There are observational signs that velocity dispersion variation indeed may play a role in observed rotation distributions of globular cluster BSSs. For example, in ω Centauri the velocity dispersion profile (A. Sollima et al. 2009) only permits main-sequence and RGB mass transfer in the core but by 3–4 times the core, radius the velocity dispersion drops sufficiently that AGB mass transfer is also possible. This is the same region where F. R. Ferraro et al. (2023) (see their Figure 5) found a fast increase in the frequency of rapid rotators.

In Paper 1, we found that very-long-period progenitor binaries ($P > 10^4$ days) must significantly contribute to the BSS population through AGB RLOF and WRLOF. Since these binaries are disrupted at most radii of globular clusters, the relative ratios of BSS formation across progenitor evolution states and even across mechanisms (e.g. mergers) could change their observed rotation distributions.

This discussion is intended only to present the idea. There remain many unaddressed issues; for example, binaries move through regions of different velocity dispersions. Ultimately, detailed binary stellar evolution models of low-mass stars coupled with N-body simulations are needed to understand relative BSS production by formation mechanism and the consequences this has for final BSS mass, T_{eff} , and rotation period.

5. SUMMARY

In this paper, we find that rotation distributions of BSSs in old open clusters show a Kraft break very similar to that found in the field. Hotter BSSs have rotation periods under two days—still well below critical velocity—which we take to trace the degree of spin-up during the formation of all BSSs in these clusters. BSSs below the Kraft break exhibit very slow rotation periods, presumably due to magnetic braking linked to their convective envelopes. BSSs within the Kraft break have a mixture of rotation rates. That these BSSs exhibit spin down only at the same temperatures at which field stars spin down indicates that at all effective temperatures they have similar structures in their envelopes even after having accreted mass from a companion. Because many known BSSs are in or hotter than the Kraft break, deriving gyrochronologic ages must be done with care.

The fraction of rapidly rotating BSSs in open clusters is directly tied to the fraction of BSSs in and above the Kraft break. In metal-poor globular clusters, we found

that stars with T_{eff} below 6896 ± 156 K were significantly spun-down in comparison to the median rotation velocity above that temperature. This rotation transition is hotter by 100-250 K at low metallicities ($[\text{Fe}/\text{H}] \sim -1.5$) than at solar metallicity. However, above this temperature the globular cluster rotation distribution shows many more slowly rotating stars than found in or above the Kraft break in open clusters.

Finally, we compare the $v \sin i$ distribution of BSSs in open and globular clusters and find that the density of formation environment is not the only possible cause for the fraction of fast and slow rotators in a cluster. For example, the local velocity dispersion at a region in a globular cluster can impact the available progenitor binaries and perhaps formation mechanisms for BSSs, which may also manifest in different $v \sin i$ distributions.

ACKNOWLEDGEMENTS

The authors express their gratitude to D. Dixon, E. Leiner, E. Motherway, R. S. Narayan, A. Nine, and R. Townsend for their insightful feedback during the creation of this manuscript and to the many undergraduate and graduate students of the R. D. Mathieu research group and the staff of WIYN observatory, without whom we would not have been able to collect thousands of stellar spectra that enabled the findings of this work. Finally, we acknowledge the support of the Wisconsin Alumni Research Fund and the Wisconsin Space Grant

Consortium through awards RFP25_4-0 and RFP25_12-0.

This work has made use of data from the European Space Agency (ESA) mission Gaia (<https://www.cosmos.esa.int/gaia>), processed by the Gaia Data Processing and Analysis Consortium (DPAC; <https://www.cosmos.esa.int/web/gaia/dpac/consortium>). Funding for the DPAC has been provided by national institutions, in particular the institutions participating in the Gaia Multilateral Agreement.

This work was conducted at the University of Wisconsin-Madison, which is located on occupied ancestral land of the Ho-Chunk people, a place their nation has called Teejop since time immemorial. In an 1832 treaty, the Ho-Chunk were forced to cede this territory. The university was founded on and funded through this seized land; this legacy enabled the science presented here. Observations for this work were conducted at the WIYN telescope on Kitt Peak, which is part of the lands of the Tohono O’odham Nation.

Facilities: WIYN - Wisconsin-Indiana-Yale-NOAO Telescope (Hydra MOS), Gaia

Software: Astropy (Astropy Collaboration et al. 2013, 2018, 2022), MIST (A. Dotter 2016; J. Choi et al. 2016; B. Paxton et al. 2011, 2013, 2015), NumPy (C. R. Harris et al. 2020), SciPy (P. Virtanen et al. 2020), scikit-learn (F. Pedregosa et al. 2011), ChatGPT-4 (OpenAI 2025)

APPENDIX

A. BSS $v \sin i$, T_{eff} , AND RADIUS MEASUREMENTS

Table 1 contains the Gaia DR3 ID, WOCS ID, and Gaia DR3 RA and Dec (Gaia Collaboration et al. 2023) of each BSSs in M67, NGC 188, and NGC 6791 along with $v \sin i$ measurements and the T_{eff} and radius found in Paper 1.

Several studies have spectroscopically measured temperatures of some of the BSSs in M67 and NGC 188. GALAH Survey DR4 (S. Buder et al. 2025; J. Kos et al. 2025) has measured the T_{eff} of 13 of the M67 BSSs; the average absolute difference between their measurements and ours is 75 K with no systematic differences and a maximum difference of 130 K. A. C. Nine et al. (2024) fit the temperatures of 15 of the M67 BSSs using the temperature-sensitive wing profiles of $\text{H}\alpha$; they found temperatures that were on average 220 K cooler than we found, with the largest deviations (600 K) among stars of $T_{\text{eff}} > 8000$ K where the $\text{H}\alpha$ technique becomes less sensitive to temperature due to Stark broadening (L. Lovisi et al. 2012). After removing any measurements flagged for bad values, APOGEE-2 has spectroscopic T_{eff} measurements of many of the hottest BSSs (7 in M67 and 2 in NGC 188, Abdurro’uf et al. 2022). These measurements are on average ~ 600 K cooler (range 370-1120 K) than MIST and GALAH DR4. Although these differences are significant, the lower temperatures do not change the temperature region of any BSSs in Section 3.1.

We note that the relationship between Gaia colors and MIST-derived T_{eff} becomes steeper above 8000 K (Gaia BP–RP < 0.2), so a small change in color leads to a larger change in temperature, which may explain some of the differences seen above.

REFERENCES

- Abate, C., Pols, O. R., Izzard, R. G., Mohamed, S. S., & De Mink, S. E. 2013, *Astronomy & Astrophysics*, 552, A26, doi: 10.1051/0004-6361/201220007
- Abdurro’uf, Accetta, K., Aerts, C., et al. 2022, *The Astrophysical Journal Supplement Series*, 259, 35, doi: 10.3847/1538-4365/ac4414

Table 1. BSS $v \sin i$, T_{eff} , and Radius Measurements

Gaia DR3 ID	WOCS ID	Cluster	RA (ICRS)	Dec (ICRS)
573933322966008960	8104	NGC 188	10.064616585556992	85.06345774998789
573937961530665088	5467	NGC 188	12.60415212043305	85.18392229634908
573944111923749760	4540	NGC 188	11.326406727485669	85.32219238013796

$v \sin i$	T_{eff}	Radius
km s ⁻¹	K	R _☉
< 10	6081 [6039, 6127]	1.11 [1.10, 1.13]
< 10	6126 [6085, 6171]	1.15 [1.13, 1.16]
70	6651 [6613, 6693]	2.29 [2.27, 2.31]

NOTE—This table is available in machine-readable format. A portion is shown here for guidance regarding its content. The first value is the average and the values in the square brackets are the value at the 16th and 84th percentiles, respectively. $v \sin i$ values below our floor are marked with < 10 km s⁻¹.

- Alvarez-Baena, N., Carrera, R., Thompson, H., et al. 2024, *Astronomy & Astrophysics*, 687, A101, doi: [10.1051/0004-6361/202348220](https://doi.org/10.1051/0004-6361/202348220)
- Amard, L., & Matt, S. P. 2020, *The Astrophysical Journal*, 889, 108, doi: [10.3847/1538-4357/ab6173](https://doi.org/10.3847/1538-4357/ab6173)
- Amard, L., Palacios, A., Charbonnel, C., et al. 2019, *Astronomy & Astrophysics*, 631, A77, doi: [10.1051/0004-6361/201935160](https://doi.org/10.1051/0004-6361/201935160)
- Amard, L., Roquette, J., & Matt, S. P. 2020, *Monthly Notices of the Royal Astronomical Society*, 499, 3481, doi: [10.1093/mnras/staa3038](https://doi.org/10.1093/mnras/staa3038)
- Andronov, N., Pinsonneault, M. H., & Terndrup, D. M. 2006, *The Astrophysical Journal*, 646, 1160, doi: [10.1086/505127](https://doi.org/10.1086/505127)
- Angus, R., Morton, T. D., Foreman-Mackey, D., et al. 2019, *The Astronomical Journal*, 158, 173, doi: [10.3847/1538-3881/ab3c53](https://doi.org/10.3847/1538-3881/ab3c53)
- Astropy Collaboration, Robitaille, T. P., Tollerud, E. J., et al. 2013, *Astronomy and Astrophysics*, 558, A33, doi: [10.1051/0004-6361/201322068](https://doi.org/10.1051/0004-6361/201322068)
- Astropy Collaboration, Price-Whelan, A. M., Sipőcz, B. M., et al. 2018, *The Astronomical Journal*, 156, 123, doi: [10.3847/1538-3881/aabc4f](https://doi.org/10.3847/1538-3881/aabc4f)
- Astropy Collaboration, Price-Whelan, A. M., Lim, P. L., et al. 2022, *The Astrophysical Journal*, 935, 167, doi: [10.3847/1538-4357/ac7c74](https://doi.org/10.3847/1538-4357/ac7c74)
- Balona, L. A. 2011, *Monthly Notices of the Royal Astronomical Society*, 415, 1691, doi: [10.1111/j.1365-2966.2011.18813.x](https://doi.org/10.1111/j.1365-2966.2011.18813.x)
- Barnes, S. A. 2003, *The Astrophysical Journal*, 586, 464, doi: [10.1086/367639](https://doi.org/10.1086/367639)
- Baumgardt, H., & Hilker, M. 2018, *Monthly Notices of the Royal Astronomical Society*, 478, 1520, doi: [10.1093/mnras/sty1057](https://doi.org/10.1093/mnras/sty1057)
- Baumgardt, H., & Vasiliev, E. 2021, *Monthly Notices of the Royal Astronomical Society*, 505, 5957, doi: [10.1093/mnras/stab1474](https://doi.org/10.1093/mnras/stab1474)
- Beyer, A. C., & White, R. J. 2024, *The Astrophysical Journal*, 973, 28, doi: [10.3847/1538-4357/ad6b0d](https://doi.org/10.3847/1538-4357/ad6b0d)
- Billi, A., Ferraro, F. R., Mucciarelli, A., et al. 2024, *Astronomy & Astrophysics*, 690, A156, doi: [10.1051/0004-6361/202450593](https://doi.org/10.1051/0004-6361/202450593)
- Billi, A., Monaco, L., Ferraro, F. R., et al. 2026, *Astronomy & Astrophysics*, 705, A36, doi: [10.1051/0004-6361/202557251](https://doi.org/10.1051/0004-6361/202557251)
- Billi, A., Ferraro, F. R., Mucciarelli, A., et al. 2023, *The Astrophysical Journal*, 956, 124, doi: [10.3847/1538-4357/acf372](https://doi.org/10.3847/1538-4357/acf372)
- Bonanno, A. M., Corsaro, E., Metcalfe, T. S., et al. 2025, *The Astrophysical Journal*, 995, 32, doi: [10.3847/1538-4357/ae12f2](https://doi.org/10.3847/1538-4357/ae12f2)
- Bouma, L. G., Hartman, J. D., Bhatti, W., Winn, J. N., & Bakos, G. A. 2019, *The Astrophysical Journal Supplement Series*, 245, 13, doi: [10.3847/1538-4365/ab4a7e](https://doi.org/10.3847/1538-4365/ab4a7e)
- Bouma, L. G., Palumbo, E. K., & Hillenbrand, L. A. 2023, *The Astrophysical Journal Letters*, 947, L3, doi: [10.3847/2041-8213/acc589](https://doi.org/10.3847/2041-8213/acc589)

- Buder, S., Kos, J., Wang, X. E., et al. 2025, *Publications of the Astronomical Society of Australia*, 42, e051, doi: [10.1017/pasa.2025.26](https://doi.org/10.1017/pasa.2025.26)
- Carney, B. W., Latham, D. W., & Laird, J. B. 2005, *The Astronomical Journal*, 129, 466, doi: [10.1086/426566](https://doi.org/10.1086/426566)
- Choi, J., Dotter, A., Conroy, C., et al. 2016, *The Astrophysical Journal*, 823, 102, doi: [10.3847/0004-637X/823/2/102](https://doi.org/10.3847/0004-637X/823/2/102)
- Dotter, A. 2016, *The Astrophysical Journal Supplement Series*, 222, 8, doi: [10.3847/0067-0049/222/1/8](https://doi.org/10.3847/0067-0049/222/1/8)
- Eggleton, P. P. 1983, *The Astrophysical Journal*, 268, 368, doi: [10.1086/160960](https://doi.org/10.1086/160960)
- Ferraro, F. R., Sabbi, E., Gratton, R., et al. 2006, *The Astrophysical Journal*, 647, L53, doi: [10.1086/507327](https://doi.org/10.1086/507327)
- Ferraro, F. R., Mucciarelli, A., Lanzoni, B., et al. 2023, *Nature Communications*, 14, 2584, doi: [10.1038/s41467-023-38153-w](https://doi.org/10.1038/s41467-023-38153-w)
- Ferraro, F. R., Lanzoni, B., Vesperini, E., et al. 2026, *Nature Communications*, 17, 768, doi: [10.1038/s41467-025-68159-5](https://doi.org/10.1038/s41467-025-68159-5)
- Fitzpatrick, M. J. 1993, in *Astronomical Data Analysis Software and Systems II*, Vol. 52, 472. <https://ui.adsabs.harvard.edu/abs/1993ASPC...52.472F>
- Gaia Collaboration, Vallenari, A., Brown, A. G. A., et al. 2023, *Astronomy and Astrophysics*, 674, A1, doi: [10.1051/0004-6361/202243940](https://doi.org/10.1051/0004-6361/202243940)
- Geller, A. M., & Leigh, N. W. C. 2015, *The Astrophysical Journal Letters*, 808, L25, doi: [10.1088/2041-8205/808/1/L25](https://doi.org/10.1088/2041-8205/808/1/L25)
- Geller, A. M., Mathieu, R. D., Braden, E. K., et al. 2010, *The Astronomical Journal*, 139, 1383, doi: [10.1088/0004-6256/139/4/1383](https://doi.org/10.1088/0004-6256/139/4/1383)
- Geller, A. M., Mathieu, R. D., Latham, D. W., et al. 2021, *The Astronomical Journal*, 161, 190, doi: [10.3847/1538-3881/abdd23](https://doi.org/10.3847/1538-3881/abdd23)
- Gosnell, N. M., Leiner, E. M., Mathieu, R. D., et al. 2019, *The Astrophysical Journal*, 885, 45, doi: [10.3847/1538-4357/ab4273](https://doi.org/10.3847/1538-4357/ab4273)
- Gosnell, N. M., Mathieu, R. D., Geller, A. M., et al. 2015, *The Astrophysical Journal*, 814, 163, doi: [10.1088/0004-637X/814/2/163](https://doi.org/10.1088/0004-637X/814/2/163)
- Gossage, S., Kalogera, V., & Sun, M. 2023, *The Astrophysical Journal*, 950, 27, doi: [10.3847/1538-4357/acc86e](https://doi.org/10.3847/1538-4357/acc86e)
- Harris, C. R., Millman, K. J., van der Walt, S. J., et al. 2020, *Nature*, 585, 357, doi: [10.1038/s41586-020-2649-2](https://doi.org/10.1038/s41586-020-2649-2)
- Harris, W. E. 1996, *The Astronomical Journal*, 112, 1487, doi: [10.1086/118116](https://doi.org/10.1086/118116)
- Hilker, M., Baumgardt, H., Sollima, A., & Bellini, A. 2019, *Proceedings of the International Astronomical Union*, 14, 451, doi: [10.1017/S1743921319006823](https://doi.org/10.1017/S1743921319006823)
- Jadhav, V. V., Sindhu, N., & Subramaniam, A. 2019, *The Astrophysical Journal*, 886, 13, doi: [10.3847/1538-4357/ab4b43](https://doi.org/10.3847/1538-4357/ab4b43)
- Jadhav, V. V., & Subramaniam, A. 2021, *Monthly Notices of the Royal Astronomical Society*, 507, 1699, doi: [10.1093/mnras/stab2264](https://doi.org/10.1093/mnras/stab2264)
- Jermyn, A. S., Bauer, E. B., Schwab, J., et al. 2023, *The Astrophysical Journal Supplement Series*, 265, 15, doi: [10.3847/1538-4365/aca8d](https://doi.org/10.3847/1538-4365/aca8d)
- Kos, J., Buder, S., Beeson, K. L., et al. 2025, *Astronomy & Astrophysics*, 703, A104, doi: [10.1051/0004-6361/202554112](https://doi.org/10.1051/0004-6361/202554112)
- Kraft, R. P. 1967, *The Astrophysical Journal*, 150, 551, doi: [10.1086/149359](https://doi.org/10.1086/149359)
- Leigh, N., Sills, A., & Knigge, C. 2007, *The Astrophysical Journal*, 661, 210, doi: [10.1086/514330](https://doi.org/10.1086/514330)
- Leiner, E., Mathieu, R. D., Gosnell, N. M., & Sills, A. 2018, *The Astrophysical Journal*, 869, L29, doi: [10.3847/2041-8213/aaf4ed](https://doi.org/10.3847/2041-8213/aaf4ed)
- Leiner, E., Mathieu, R. D., Vanderburg, A., Gosnell, N. M., & Smith, J. C. 2019, *The Astrophysical Journal*, 881, 47, doi: [10.3847/1538-4357/ab2bf8](https://doi.org/10.3847/1538-4357/ab2bf8)
- Leiner, E. M., & Geller, A. 2021, *The Astrophysical Journal*, 908, 229, doi: [10.3847/1538-4357/abd7e9](https://doi.org/10.3847/1538-4357/abd7e9)
- Leiner, E. M., Gosnell, N. M., Geller, A. M., et al. 2025, *The Astrophysical Journal Letters*, 979, L1, doi: [10.3847/2041-8213/ad9d0c](https://doi.org/10.3847/2041-8213/ad9d0c)
- Leonard, P. J. T. 1989, *The Astronomical Journal*, 98, 217, doi: [10.1086/115138](https://doi.org/10.1086/115138)
- Linck, E., & Mathieu, R. D. 2026, *The Distribution of Blue Straggler Stars in the Color-Magnitude Diagrams of Old Open Clusters*, arXiv, doi: [10.48550/arXiv.2605.14187](https://doi.org/10.48550/arXiv.2605.14187)
- Linck, E., Mathieu, R. D., & Latham, D. W. 2024, *The Astronomical Journal*, 168, 205, doi: [10.3847/1538-3881/ad6b1a](https://doi.org/10.3847/1538-3881/ad6b1a)
- Lovisi, L., Mucciarelli, A., Dalessandro, E., Ferraro, F. R., & Lanzoni, B. 2013a, *The Astrophysical Journal*, 778, 64, doi: [10.1088/0004-637X/778/1/64](https://doi.org/10.1088/0004-637X/778/1/64)
- Lovisi, L., Mucciarelli, A., Lanzoni, B., et al. 2013b, *The Astrophysical Journal*, 772, 148, doi: [10.1088/0004-637X/772/2/148](https://doi.org/10.1088/0004-637X/772/2/148)
- Lovisi, L., Mucciarelli, A., Lanzoni, B., et al. 2012, *The Astrophysical Journal*, 754, 91, doi: [10.1088/0004-637X/754/2/91](https://doi.org/10.1088/0004-637X/754/2/91)
- Lovisi, L., Mucciarelli, A., Ferraro, F. R., et al. 2010, *The Astrophysical Journal*, 719, L121, doi: [10.1088/2041-8205/719/2/L121](https://doi.org/10.1088/2041-8205/719/2/L121)

- Lurie, J. C., Vyhmeister, K., Hawley, S. L., et al. 2017, *The Astronomical Journal*, 154, 250, doi: [10.3847/1538-3881/aa974d](https://doi.org/10.3847/1538-3881/aa974d)
- Mathieu, R. D. 2000, *Stellar Clusters and Associations: Convection, Rotation, and Dynamos*. Proceedings from ASP Conference, 198, 517. <https://ui.adsabs.harvard.edu/abs/2000ASPC..198..517M>
- Mathieu, R. D., & Pols, O. R. 2025, *Annual Review of Astronomy and Astrophysics*, 63, 467, doi: [10.1146/annurev-astro-071221-054402](https://doi.org/10.1146/annurev-astro-071221-054402)
- Matrozis, E., Abate, C., & Stancliffe, R. J. 2017, *Astronomy and Astrophysics*, 606, A137, doi: [10.1051/0004-6361/201730746](https://doi.org/10.1051/0004-6361/201730746)
- McCrea, W. H. 1964, *Monthly Notices of the Royal Astronomical Society*, 128, 147, doi: [10.1093/mnras/128.2.147](https://doi.org/10.1093/mnras/128.2.147)
- Mucciarelli, A., Lovisi, L., Ferraro, F. R., et al. 2014, *The Astrophysical Journal*, 797, 43, doi: [10.1088/0004-637X/797/1/43](https://doi.org/10.1088/0004-637X/797/1/43)
- Narayan, R. S., Linck, E., Mathieu, R. D., & Geller, A. M. 2026, *The Astronomical Journal*, 171, 102, doi: [10.3847/1538-3881/ae2d14](https://doi.org/10.3847/1538-3881/ae2d14)
- Nine, A. C., Mathieu, R. D., Gosnell, N. M., & Leiner, E. M. 2023, *The Astrophysical Journal*, 944, 145, doi: [10.3847/1538-4357/acb046](https://doi.org/10.3847/1538-4357/acb046)
- Nine, A. C., Mathieu, R. D., Schuler, S. C., & Milliman, K. E. 2024, *The Astrophysical Journal*, 970, 187, doi: [10.3847/1538-4357/ad534b](https://doi.org/10.3847/1538-4357/ad534b)
- OpenAI. 2025, ChatGPT-4, ChatGPT-4. chatgpt.com
- Packet, W. 1981, *Astronomy and Astrophysics*, 102, 17. <https://ui.adsabs.harvard.edu/abs/1981A&A...102...17P>
- Pal, H., Subramaniam, A., Reddy, A. B. S., & Jadhav, V. V. 2024, *The Astrophysical Journal Letters*, 970, L39, doi: [10.3847/2041-8213/ad6316](https://doi.org/10.3847/2041-8213/ad6316)
- Pancino, E., Zocchi, A., Rainer, M., et al. 2024, *Astronomy & Astrophysics*, 686, A283, doi: [10.1051/0004-6361/202449462](https://doi.org/10.1051/0004-6361/202449462)
- Paxton, B., Bildsten, L., Dotter, A., et al. 2011, *The Astrophysical Journal Supplement Series*, 192, 3, doi: [10.1088/0067-0049/192/1/3](https://doi.org/10.1088/0067-0049/192/1/3)
- Paxton, B., Cantiello, M., Arras, P., et al. 2013, *The Astrophysical Journal Supplement Series*, 208, 4, doi: [10.1088/0067-0049/208/1/4](https://doi.org/10.1088/0067-0049/208/1/4)
- Paxton, B., Marchant, P., Schwab, J., et al. 2015, *The Astrophysical Journal Supplement Series*, 220, 15, doi: [10.1088/0067-0049/220/1/15](https://doi.org/10.1088/0067-0049/220/1/15)
- Paxton, B., Schwab, J., Bauer, E. B., et al. 2018, *The Astrophysical Journal Supplement Series*, 234, 34, doi: [10.3847/1538-4365/aaa5a8](https://doi.org/10.3847/1538-4365/aaa5a8)
- Paxton, B., Smolec, R., Schwab, J., et al. 2019, *The Astrophysical Journal Supplement Series*, 243, 10, doi: [10.3847/1538-4365/ab2241](https://doi.org/10.3847/1538-4365/ab2241)
- Pedregosa, F., Varoquaux, G., Gramfort, A., et al. 2011, *Journal of Machine Learning Research*, 12, 2825
- Preston, G. W., & Sneden, C. 2000, *The Astronomical Journal*, 120, 1014, doi: [10.1086/301472](https://doi.org/10.1086/301472)
- Rhode, K. L., Herbst, W., & Mathieu, R. D. 2001, *The Astronomical Journal*, 122, 3258, doi: [10.1086/324448](https://doi.org/10.1086/324448)
- Sanjayan, S., Baran, A., Németh, P., et al. 2022, *Acta Astronomica*, 72, 77, doi: [10.32023/0001-5237/72.2.1](https://doi.org/10.32023/0001-5237/72.2.1)
- Schlafly, E. F., & Finkbeiner, D. P. 2011, *The Astrophysical Journal*, 737, 103, doi: [10.1088/0004-637X/737/2/103](https://doi.org/10.1088/0004-637X/737/2/103)
- Schneider, F. R. N., Ohlmann, S. T., Podsiadlowski, P., et al. 2019, *Nature*, 574, 211, doi: [10.1038/s41586-019-1621-5](https://doi.org/10.1038/s41586-019-1621-5)
- Sills, A., Adams, T., & Davies, M. B. 2005, *Monthly Notices of the Royal Astronomical Society*, 358, 716, doi: [10.1111/j.1365-2966.2005.08809.x](https://doi.org/10.1111/j.1365-2966.2005.08809.x)
- Sills, A., Adams, T., Davies, M. B., & Bate, M. R. 2002, *Monthly Notices of the Royal Astronomical Society*, 332, 49, doi: [10.1046/j.1365-8711.2002.05266.x](https://doi.org/10.1046/j.1365-8711.2002.05266.x)
- Sindhu, N., Subramaniam, A., Jadhav, V. V., et al. 2019, *The Astrophysical Journal*, 882, 43, doi: [10.3847/1538-4357/ab31a8](https://doi.org/10.3847/1538-4357/ab31a8)
- Skipper, S., & Josef, P. 2010, 9th Python in Science Conference
- Sollima, A., Bellazzini, M., Smart, R. L., et al. 2009, *Monthly Notices of the Royal Astronomical Society*, 396, 2183, doi: [10.1111/j.1365-2966.2009.14864.x](https://doi.org/10.1111/j.1365-2966.2009.14864.x)
- Sollima, A., Lanzoni, B., Beccari, G., Ferraro, F. R., & Fusi Pecci, F. 2008, *Astronomy and Astrophysics*, 481, 701, doi: [10.1051/0004-6361:20079082](https://doi.org/10.1051/0004-6361:20079082)
- Spalding, C., & Winn, J. N. 2022, *The Astrophysical Journal*, 927, 22, doi: [10.3847/1538-4357/ac4993](https://doi.org/10.3847/1538-4357/ac4993)
- Stetson, P. B., Pancino, E., Zocchi, A., Sanna, N., & Monelli, M. 2019, *Monthly Notices of the Royal Astronomical Society*, 485, 3042, doi: [10.1093/mnras/stz585](https://doi.org/10.1093/mnras/stz585)
- Sun, M., Gossage, S., Leiner, E. M., & Geller, A. M. 2024a, *The Astrophysical Journal*, 971, 80, doi: [10.3847/1538-4357/ad54be](https://doi.org/10.3847/1538-4357/ad54be)
- Sun, M., Levina, S., Gossage, S., et al. 2024b, *The Astrophysical Journal*, 969, 8, doi: [10.3847/1538-4357/ad47c1](https://doi.org/10.3847/1538-4357/ad47c1)
- Tofflemire, B. M., Gosnell, N. M., Mathieu, R. D., & Platais, I. 2014, *The Astronomical Journal*, 148, 61, doi: [10.1088/0004-6256/148/4/61](https://doi.org/10.1088/0004-6256/148/4/61)

Van-Lane, P. R., Speagle, J. S., Eadie, G. M., et al. 2025, The Astrophysical Journal, 986, 59, doi: [10.3847/1538-4357/adcd73](https://doi.org/10.3847/1538-4357/adcd73)

Vernekar, N., Subramaniam, A., Jadhav, V. V., & Bowman, D. M. 2023, Monthly Notices of the Royal Astronomical Society, 524, 1360, doi: [10.1093/mnras/stad1947](https://doi.org/10.1093/mnras/stad1947)

Virtanen, P., Gommers, R., Oliphant, T. E., et al. 2020,

Nature Methods, 17, 261, doi: [10.1038/s41592-019-0686-2](https://doi.org/10.1038/s41592-019-0686-2)